How solute size and charge influence osmosis

James Cannon,*,† Daejoong Kim,‡ Shigeo Maruyama,† and Junichiro Shiomi*,†

Department of Mechanical Engineering, The University of Tokyo, 7-3-1 Hongo, Bunkyo-ku, Tokyo 113-8656, Japan, and Department of Mechanical Engineering, Sogang University, 505 Adam Schall Hall, 1 Shinsu-dong, Mapo-gu, Seoul, 121-742, Republic of Korea

E-mail: cannon@photon.t.u-tokyo.ac.jp; shiomi@photon.t.u-tokyo.ac.jp

Abstract

Osmosis is fundamental to many processes, such as in the function of biological cells and in industrial desalination to obtain clean drinking water. The choice of solute in industrial applications of osmosis is highly important in maximising efficiency and minimising costs. The macro-scale process of osmosis originates from the nano-scale properties of the solvent, and therefore an understanding of the mechanisms of how these properties determine osmotic strength can be highly useful. For this reason we have undertaken molecular dynamics simulations to systematically study the influence of ion size and charge on the strength of osmosis of water through carbon nanotube membranes. Our results show that strong osmosis occurs under optimum conditions of ion placement near the region of high water density near the membrane wall, and maintenance of a strong water hydration shell around the ions. The results in turn allow greater insight into the origin of the strong osmotic strength of real ions such as NaCl. Finally, in terms of practical simulation, we highlight the importance of avoiding size effects that can occur if the simulation cell is too small.

*To whom correspondence should be addressed
†The University of Tokyo
‡Sogang University

Introduction

Osmosis is a fundamental process in a wide range of biological and industrial processes. For example, osmosis is the mechanism by which cells in plants, animals and humans maintain their volume.[1] The impact of osmosis on life can also be indirect, whether for example in terms of factory processes[2] or membrane-based desalination methods for clean drinking water.[3,4]

Given the prevalence of osmosis in such a wide range of key processes, it is important to have a detailed understanding of the phenomenon, so that industrial processes can be optimised and biological functions be better understood. This is particularly the case for applications such as desalination, where membrane-based reverse-osmosis methods have recently overtaken thermal techniques in popularity,[4] and there is a growing interest in forward osmosis methods which require a strong osmotic pressure-gradient.

Although the effect of osmosis can be observed on the macro-scale, the process originates through interactions between molecules, and therefore nano-scale simulation can offer detailed insight into the fundamentals of this process. For this reason, a number of simulation studies have explored this phenomenon. For example, Kalra et. al.[5] studied osmosis through a membrane made of carbon nanotubes by way of molecular dynamics (MD) simulation. Nanotubes are a particularly promising form of membrane for osmotic applications, due to their relatively smooth inner structure, and the potential flow rates which are higher than than conventional theory would predict.[6–9] Corry[10] also used MD simulation to demonstrate the potential effectiveness of nanotubes in achieving significant osmosis for application in desalination technologies, and more recently Jia et al.[9] demonstrated that the strong selectivity of nanotubes coupled with high flow rates may make them ideal for forward-osmosis applications. Beyond studies of nanotube membranes, the MD simulation method has been shown to be effective and accurate in reproducing osmosis across a range of membranes, whether for very simple fundamental systems,[11,12] or for complex reproductions of existing membranes.[13,14]

Central to the process of osmosis is the solute itself. The type of solute dictates the rate of osmosis, and therefore in industrial applications it is a crucial element in achieving high efficiency.

Raghunathan et al.[15] for example, found that the rate of osmosis using NaCl as the drawing solute is different to when KCl is used, and suggested that this was because of the differing affinities of the ions to the membrane, as well as the hydration of the ions. It remains unclear however to what extent the different atomic properties such as size and charge influence the osmosis, and how the inter-relation of ion and water positioning effects the osmosis. This is important when considering what the "ideal" solute might be for a given application.

We have therefore undertaken a systematic simulation study to gauge the effect of solute size and charge on osmotic strength. By making this study, it is our intention to give a greater understanding of what solute qualities effect osmotic strength, and help guide decisions about drawing solutes to increase the efficiency of osmosis-based processes and applications.

Simulation design

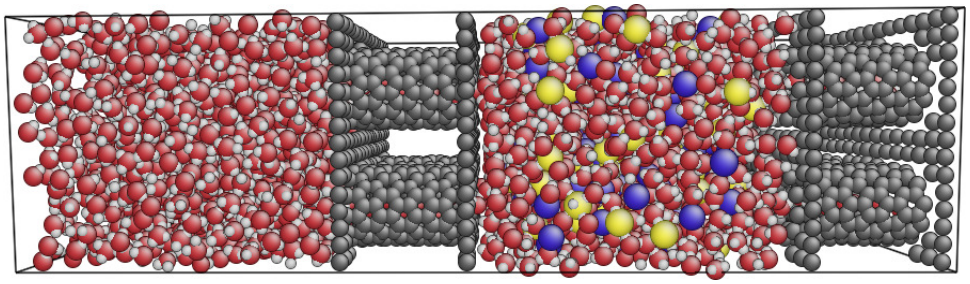

Figure 1: A representative snapshot of the simulation system

The system design is shown in figure Figure 1. The left chamber contains pure water (PW), whilst the right chamber consists of a salt-water (SW) solution, initially at 5M concentration. These are separated by a square 2x2 array carbon nanotube membrane (4 nanotubes in each membrane, 8 nanotubes in total in the system), with each nanotube of chirality (11,0) and diameter 8.6Å. The nanotubes have a length of 15Å, while the length of each chamber is around 45Å. The lateral x and y dimensions are 30Å each. Periodic boundary conditions are employed so the nanotube membranes are essentially infinite, whilst water is able to flow both left and right between the chambers.

Initially the system is equilibrated for 4ns. During this time, through the process of osmosis, some water flows from the pure-water chamber on the left to the salt-water chamber on the right. This causes a decrease in the hydrostatic pressure in the pure-water chamber and a corresponding increase in the salt-water chamber. Despite allowing the pressure in each individual chamber to vary in this manner, in order to maintain comparability between simulations, the net pressure is maintained constant. This can be understood through Eq. (1), when denoting the hydrostatic pressure experienced on the left and right walls of the PW chamber as P_{W1} and P_{W2} respectively, and that on the walls of the SW chamber as P_{W3} and P_{W4} in the same respect.

$$\frac{P_{W1}+P_{W2}}{2}+\frac{P_{W3}+P_{W4}}{2}=K_P \tag{1}$$

The way that this net constant pressure is maintained during equilibration across all simulations, is to vary the length of each chamber. Even when accounting for the full range of ion radii considered in this study, the chamber lengths do not change more than 5Å from the initial 45Å length. The length of the PW and SW chambers are varied in tandem, and therefore are equal at all times. It is in principle possible to define the constant K_P in Eq. (1) in terms of average pressure on the walls of each chamber, or in terms of the average force on the walls, K_F, which can then be converted to K_P if required by dividing by the available wall area. We choose to use the latter definition, K_F, since the wall force is directly measurable within MD simulation, and there are inherent difficulties in defining surface area and local pressure at such small scales and in such confined geometries. The value of the constant force K_F is set to be 1.674kJ which corresponds to a prescribed density of $1055 kg/m^3$ in each chamber.

The choice of force constant K_F, or its equivalent in terms of pressure K_P, is a result of the desire for the prescribed high density in each chamber in order to force water into the nanotubes. This density does not vary significantly throughout the simulations, since the number of water molecules required to flow between the chambers, in order to establish a hydrostatic-pressure osmotic-pressure equilibrium, is relatively small in this small system. Although this density suggests a relatively high pressure, our tests show that it represents one of the minimum densities (ie,

minimum pressures) required for entry of water into carbon nanotubes of this diameter.

This high-density/pressure approach is common in such MD salt-water studies which consider such small nanotubes, since it is necessary to generate flow through the nanotubes.[10,16] For example, Raghunathan et. al.[15] have an initial water density of around $1200 kg/m^3$ in their lower-concentration chamber (in addition to 0.3M of salt) which, considering the relative incompressibility of water, will induce a significantly higher pressure than the one used here. Interestingly, the measured pressure in the study of Raghunathan et. al. is only 40 bar in each chamber, which would normally correspond to much lower densities of (pure) water, and this highlights the difficulties of defining pressure on the nano-scale. Nevertheless, it is notable that such a density is required to induce flow through these small nanotubes, with the implications that this carries for applications making use of such nanotubes.

As the system equilibrates, the hydrostatic pressure across the membranes will grow to oppose the osmotic pressure, until the two are in balance. Following this equilibration, the walls are fixed in their final settled position, and the strength of this wall-force difference between the two chambers is measured in order to give an indication of the osmotic strength. Due to the relatively small size, the system is sensitive to thermal fluctuations, and therefore in order to ensure accuracy, long measurements over 32ns are performed for each ion radius studied.

Interactions between atoms are governed by Lennard-Jones (LJ) interactions (Eq. (2)) and/or coulomb charge interactions. Carbon parameters are derived from water interaction with graphite,[17] both for the rigid carbon nanotubes and the simple membrane wall. For all cross-species interactions the Lorenzt-Berthelot rules[18] are applied. The parameters for the salt are based upon Sodium (Na) and Chlorine (Cl),[19,20] however in order to isolate and systematically examine the effect of changing solute radius, hypothetical ions with properties modified from standard NaCl are used. Since ε is the same for both ions, this remains at 0.4184 kJ/mol throughout the study. The mass for each ion is meanwhile set to 30 amu, which is roughly halfway between that of Na and Cl. Variation of the size of the ions is achieved by altering σ , however while Na and Cl usually have different values of σ, here $\sigma = \sigma_{Na} = \sigma_{Cl}$ unless stated otherwise, in order to isolate the effects of

specific ion radii. Therefore unless otherwise stated, for any given simulation, the only difference between the two ion species is that the Na is positive and Cl is negative. The magnitude of the charge for any given radius remains unchanged from the original value for real NaCl of $\pm 1e$.

$$V(r) = 4\varepsilon \left[\left(\frac{\sigma}{r} \right)^{12} - \left(\frac{\sigma}{r} \right)^{6} \right] \tag{2}$$

The open-source software LAMMPS[21] was used for running the MD simulations. A cut-off of 10Å was utilised for short-range LJ interactions, while Particle-Particle Particle-Mesh (PPPM)[22] methods were used to treat the long-range coulombic forces. The SPC/E model[23] was used to represent water, and a time-step of 2fs was utilised during all simulations. This time-step was found to be sufficiently small to maintain good energy conservation throughout the long simulations, whilst minimising the computational time required.

Solute size

In order to have a reference for the osmotic strength of the system, the osmosis-induced pressure difference between the chambers, dP_{real}, is calculated for the case of real NaCl ($\sigma_{Na} = 2.583$Å, $\sigma_{Cl} = 4.401$Å, $\varepsilon_{Na} = \varepsilon_{Cl} = 0.4184$ kJ/mol,[19,20] where the ions also have their normal mass and charge). Then when measuring the pressure-difference between the chambers for the hypothetical radius-controlled ions, the relative pressure difference dP_{rel} can be calculated in the fashion $dP_{rel} = dP_{this\_radius}/dP_{real}$ where $dP = P_{SW} - P_{PW}$. By using relative values, pressure can be discussed without concern over the accuracy of force-pressure conversion. The value of dP_{rel} for ion radii between 2Å and 5Å is shown in Figure 2. Radii above 5Å were also tested, but in these cases ions concentrated significantly at the membrane walls resulting in increasing water-ion separation, and it was impossible to obtain a reliable measurement of the pressure difference. This phenomenon of separation is discussed in more detail in the following paragraphs.

Figure 2 shows clearly that the medium radii, centred about 3.5~4Å, induce strongest osmosis, while that at 2Å and 5Å is remarkably weak. In order to examine the reasons behind this, it is

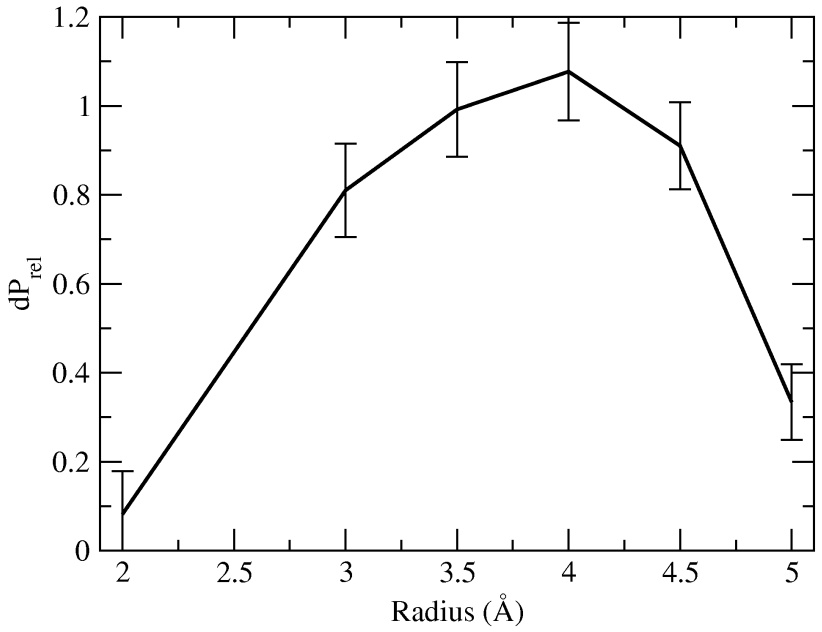

Figure 2: Relative variation of osmotic pressure with ion radius. Error-bars indicate one standard deviation.

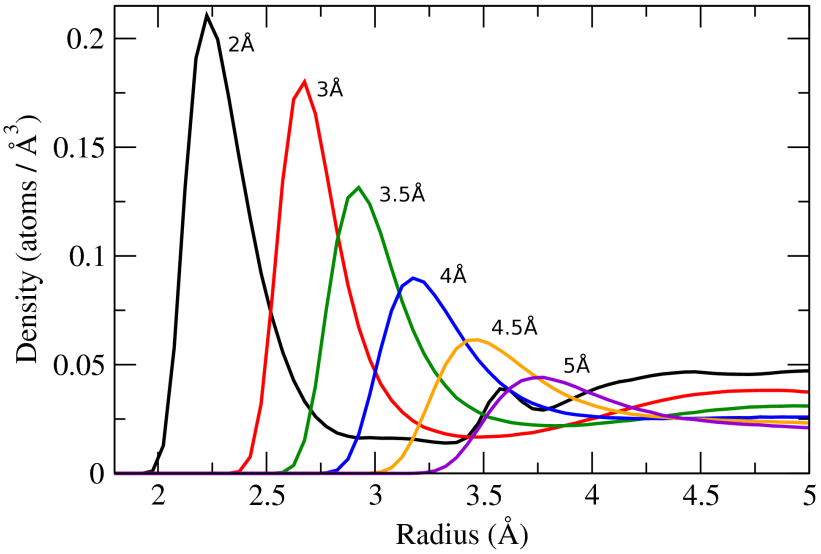

Figure 3: Variation in radial density of water around the Na ion in the salt-water chamber, for different ion radii. The peak density of water is seen to decrease as the ion-radius increases. A similar variation is observed for the Cl ion.

instructive to consider the interaction of the ions with water (Figure 3). The graph shows that as the solute radius increases, the peak density of water around the ions decreases. This is intuitive, since as the water is able to approach more closely to the ions, the coulomb interaction becomes stronger and therefore water is more tightly (and more densely) bound. Since osmosis occurs on the basis of this coulomb attraction of water to ions, the strongest osmosis would also be expected to occur for the smallest ions which pull on the water most strongly, however this has been observed not to be the case. As the following paragraphs explain, this is because the hydration of the ions not only effects their interaction strength, but also their position in the SW chamber.

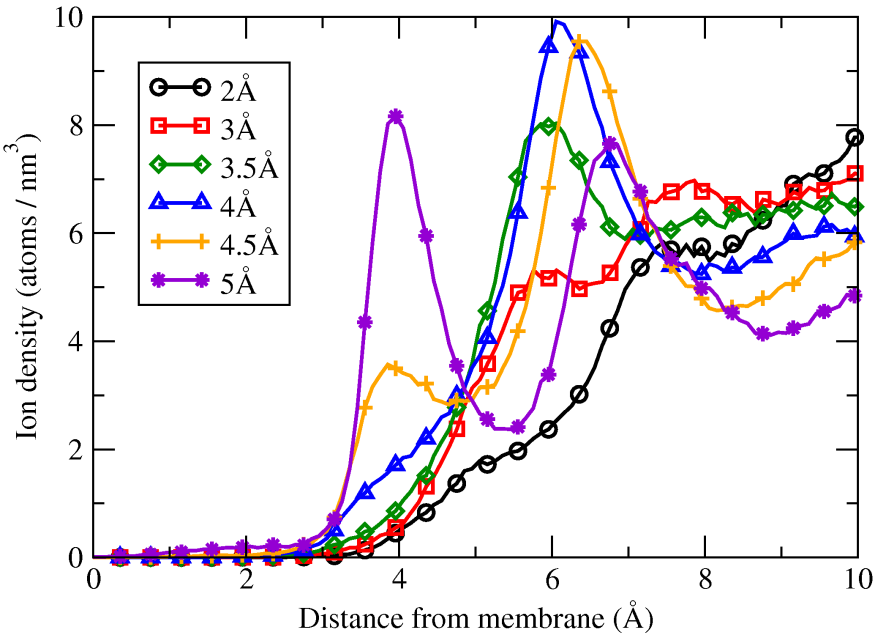

Figure 4: Variation of ion density (Na + Cl) with distance from the nanotube membrane. As the solute size increases, the density near the membrane also increases. Values are an average from the left and right walls of the SW chamber.

As the binding of water to the ions becomes weaker with increasing ion radius, the ions can be observed to be increasingly positioned towards the membrane wall (Figure 4). This can be understood in two ways. Firstly, for the ions to approach to the membrane wall it is necessary to reduce the number of water molecules in the hydration shell between the ion and the wall, and this is easiest to do with the largest ions due to the relatively weak binding between the two (the size of the hydration shell is more important for the positioning of the ion than any effect induced by the

size of the ion itself). Secondly, the larger the ion, the more hydrophobic it effectively is, as the strength of the coulomb interaction with water drops, leading to increasing ion-water separation. This is why for radii greater than 5Å it became impossible to accurately measure the pressure, as ions and water were increasingly separated, with the former increasingly by the walls and the latter increasingly in the centre of the chamber.

The 2Å ion system also experiences water-ion separation to some extent, but in contrast to the large radii where it was the weakening water-ion interaction which led to the separation, here it is the increasing ion-ion interaction which is driving the separation. This causes an asymmetry in the distribution of the ions in the SW chamber as the collection of ions is weakly attracted to one of the two membrane walls at random. So the osmosis between 2Å and 5Å can be seen in the context of a transition between the two extremes of more-hydrophilic and more-hydrophobic ions. Indeed in the extreme case where the charge on the ions is simply turned off, the ions are forced into the nanotubes while the water forms an energetically-favourable structure in the centre of each chamber. It can be noted that the bare ions are small enough to enter the nanotubes, and it is only the binding of the water in the form of a hydration shell which increases their effective size and prevents them from entering.

It has already been noted how, for the ions to induce a strong osmotic pressure, they need to pull water into the SW chamber by attracting water through coulomb interaction. One can expect this is most effectively performed when this attractive force is concentrated near the membrane itself, since movement of water from a location near the membrane deeper into the SW chamber is more encouraging of osmotic flow, compared to the movement of water already situated deep inside the chamber. Furthermore, any short-lived hydrogen-bonds may enhance osmosis by transferring the movement of water near the membrane on to water further back, or even inside the nanotubes themselves.

Figure 5 shows how, as a consequence of their position, the application of force by the smallest ions is concentrated further from the membrane wall compared to other ions. This means that despite the strong interaction with water, the contribution to osmosis is relatively ineffective, re-

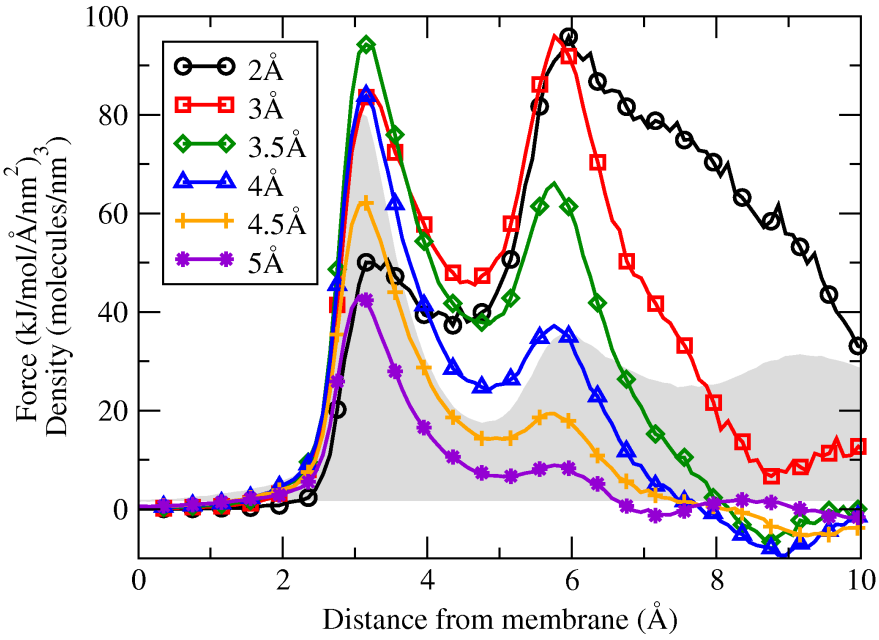

Figure 5: Lines: coulomb force by ions on water, per cross-sectional area. Shaded area: Density of water. Due to the relative densities of the ions and water, the greatest application of osmotic pull by the ions can be seen to occur at 3Å, and to a lesser extent at 6Å.

sulting in the low osmotic pressure observed. In contrast, while the largest ions do have their peak application of force near the membrane wall, this force is relatively weak. This arises for two reasons: firstly, their weak hydration results in weak pull on the water, and secondly, the very close positioning of the ions to the wall is not optimum for pulling water towards the centre of the chamber; particularly that at the peak water density at 3Å. The strong osmosis experienced by the medium radii can therefore be understood as a result of optimum positioning of ions for application of force on water near the membrane wall (particularly on water at the 3Å peak density), whilst still maintaining relatively strong hydration.

Relation of solute size to charge and the influence on osmosis

Having observed the influence of solute size on osmosis, it is interesting to consider another key variable that describes the properties of salts: the charge. For real-world osmosic applications, the drawing solution can utilise ions with single charge such as NaCl, or indeed double-charge such

as $Mg_2 + Cl_2$,[24] and it is interesting to consider coupling between optimum charge and optimum solute radius, since both influence the hydration of the ions and their subsequent position.

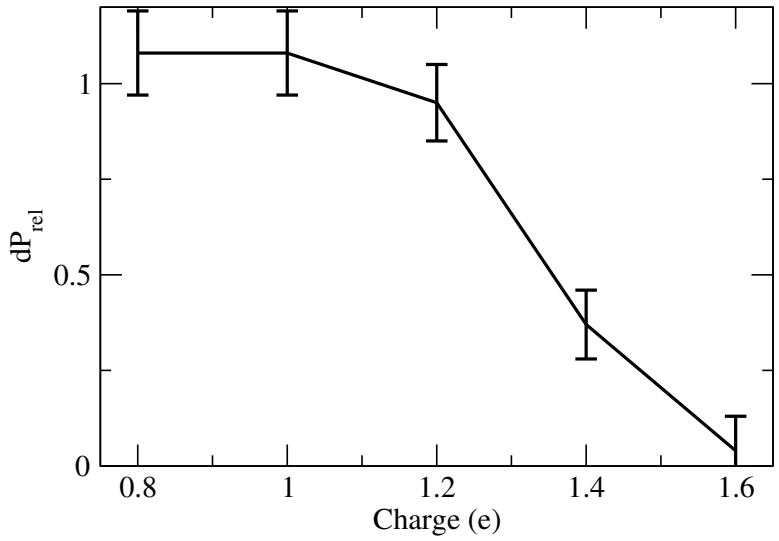

Figure 6: Relative osmotic pressure induced for the 4Å ion system as a function of charge on the ions. 0.6e charge was found to leak ions from the SW chamber to the PW chamber, preventing osmosis. Charge around 1e can be seen to be optimum for this 4Å case.

In order to investigate this, the ions radius of 4Å is considered, and the magnitude of the charge on the ions is varied. In each case, the magnitude of the charge on the positive and negative ions is the same. Figure 6 shows the transition in the strength of the osmosis with charge. For charges of 0.6e, the ions lose enough of their hydration shell that they're able to pass to the PW chamber, leading to a breakdown in the osmotic process. It was noted earlier how ions with no charge fill the nanotubes at the expense of the water, which is in contrast to the lightly charged ions passing through to the PW chamber. Therefore the mechanism of breakdown of osmosis for lightly-charged and no-charge ions is somewhat different, even while the result (ie, no osmosis) is the same.

The transition between a strong osmotic pressure at 0.8e and ion leakage at 0.6e is very sharp, while a more gradual decline in osmotic pressure is observed for strong charges. As the charge becomes stronger the ion-ion interaction becomes more predominant; like the case of the 2Å ions, the effective hydrophilicity is increasing, albeit this time due to the increase in charge, rather than the decrease in radius, and just as was the case with the small 2Å/1e ions, this leads to a drop in the osmotic pressure induced. Thus it can be understood that the hydrophilicity of the ions is

the defining factor in the effectiveness of the osmosis, and this hydrophilicity is defined through a balance of the ion size and charge. So ~1e represents the ideal charge for ions of 4Å in radius, and it can be expected that smaller ions have a lower optimum charge, while larger ions have a greater optimum charge.

Application to real-world solutes

Having gained an understanding of how size and charge alter osmosis for the hypothetical ions in this study, one can appreciate the inter-play between Na and Cl in real-world solutes, and understand how this effects osmosis. For the case of NaCl, upon which this study has its basis, the radii of the Na and Cl ions are 2.583Å and 4.401Å respectively, while they both carry $\pm$1e charge, resulting in an osmotic pressure which is similar in strength to that observed for the medium radii studied here. Using the 4Å radius ion for comparison, while the hydration of the ions for real NaCl does not differ, the slightly different distribution of the ions in the chamber reveals useful information about the mechanism leading to osmosis for this solute.

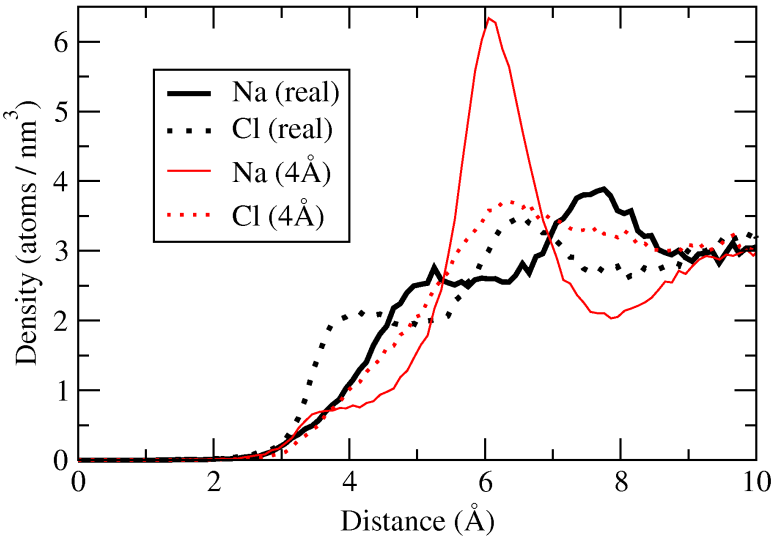

Figure 7: Ion density as a function of distance from the membrane wall, for real NaCl, and for the 4Å-radius case.

Figure 7 shows how the system with real NaCl actually allows slightly closer approach to the

membrane wall than in the 4Å case. The fact that real-Cl approaches most closely to the membrane is expected, since its radius is the largest, and it was shown earlier how larger radii approach more closely to the membrane. The closer approach of real Na to the membrane is less expected, and this arises through Na-Cl interaction: due to its small size and enhanced interaction with other atoms, the peak density of real Na around real Cl is 1.6 times higher than that measured for the 4Å case, and this, coupled with the fact that the density of Na is similar to Cl at all distances, suggests that the Na-Cl coupling is helping Na approach closer to the membrane than it otherwise would do.

The peak density of real NaCl is also observed at around 6Å, albeit with a lower peak value. This can be understood to be a consequence of the NaCl coupling, leading to an overall smoother distribution of ions. The lower peak density of ions could be expected to reduce the pull on the water, but at the same time the small Na ion, placed unusually close to the membrane due to coupling with Cl, has an increased influence on water at the membrane. The overall force on the water therefore is similar to that of the 4Å ions, and the net osmotic pressure ultimately remains the same. Thus through comparison to the hypothetical ions it is possible to gain an insight into the role of ion size and interaction which lead to the observed osmotic strength of real NaCl.

Conclusion

The molecular mechanisms of osmosis and the influence of ion size and charge have been explored, with the aim of gaining a clearer understanding of how the choice of solute determines the strength of osmosis.

By utilising hypothetical ions of various sizes, we have demonstrated that the strongest osmosis occurs for ions of around 3~4Å radius. This has been shown to arise through their optimal placement relative to water near the membrane wall, whilst maintaining reasonably strong ion-water hydration. This has in turn allowed a greater understanding of the role of inter-ion interaction and positioning in achieving strong osmosis with real NaCl.

Furthermore, by studying the effect of ion charge on osmotic strength, it has been shown that

both the charge and the size of the ion are simply mechanisms for defining the ion hydrophilicity, which is ultimately what determines the strength of the osmosis.

Overall, these results demonstrate that the osmotic strength of a solute can be highly sensitive to small changes in ion size and charge, and that careful choice of ions for forward or reverse osmosis applications can significantly enhance the efficiency of such processes.

Appendix A: Size-effects in MD

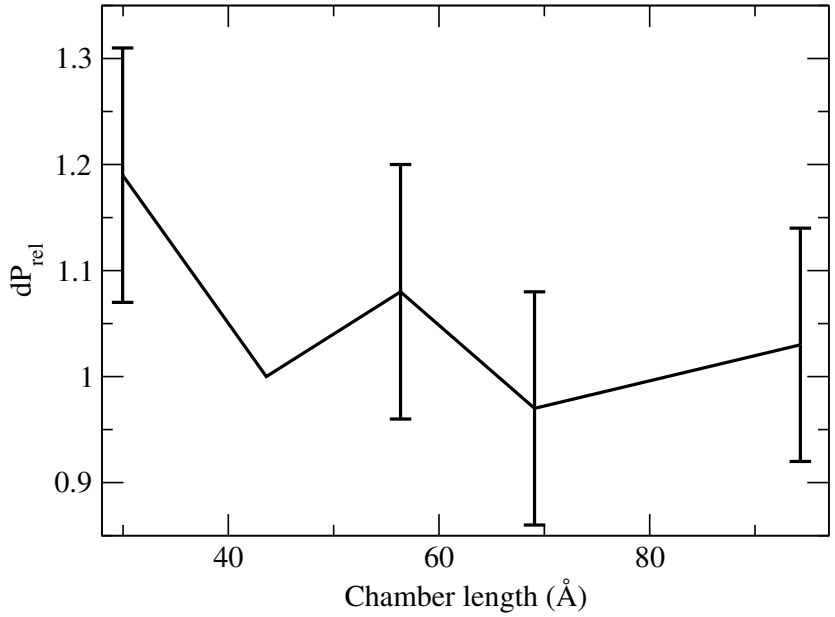

Figure 8: Osmotic pressure as a function chamber length (SW and PW) for 4Å-radius ions, relative to the osmotic pressure measured for the 43.6Å chamber used in these studies. Cross-axial dimensions are constant at 30Å each. For a chamber length of 30Å, the density of the system is notably different to the larger chambers, leading to an increase in osmotic pressure.

The simulations here make use of a chamber of approximately 45Å in length. In many simulations which consider ionic phenomena such as osmosis however, a chamber-length of 30Å is typically used.[15,25,26] In conducting such simulations it is desirable to use a chamber size which is as small as possible, in order to reduce computational cost, whilst maintaining a chamber which is large enough to be free of size-effects so that the results can be extended to macro-scale applications and experiments. In order check for any size effects, the osmotic strength of a system with

4Å ions was checked as a function of the length of the chamber (Figure 8). The results indicate a slightly larger osmotic pressure at 30Å, while at 45Å and above the osmotic pressure is consistent to within 1 standard deviation.

Further analysis of the 30Å and 45Å cases reveals that while the hydration of the ions and relative positioning of the ions do not change significantly, a slightly denser chamber is required in the case of the 30Å chamber in order to achieve the same force on the walls measured at 45Å and above. Therefore even though the relative positioning of the ions in all chambers is the same, the number of ions per unit z-axis length is slightly higher in the 30Å case, leading to an increase in the net pull of the ions on water and an increase in the osmotic pressure for the 30Å chamber.

Acknowledgement

This work is financially support in part by the Japan Society for the Promotion of Science (JSPS, project 2200064) (JC and SM), and Mukai Science and Technology Foundation (JS).

References

[1] Lang, F.; Busch, G. L.; Ritter, M.; Volkl, H.; Waldegger, S.; Gulbins, E.; Haussinger, D. *Physiological Reviews* **1998**, *78*, 247–306.

[2] Dolar, D.; Kosutic, K.; Vucic, B. *Desalination* **2011**, *265*, 237–241.

[3] McCutcheon, J. R.; McGinnis, R. L.; Elimelech, M. *Desalination* **2005**, *174*, 1–11.

[4] research council, N. *Desalination: A national perspective*; National Research Council, 2008.

[5] Kalra, A.; Garde, S.; Hummer, G. *Proceedings Of The National Academy Of Sciences Of The United States Of America* **2003**, *100*, 10175–10180.

[6] Majumder, M.; Chopra, N.; Andrews, R.; Hinds, B. J. *Nature* **2005**, *438*, 44–44.

[7] Holt, J. K.; Park, H. G.; Wang, Y. M.; Stadermann, M.; Artyukhin, A. B.; Grigoropoulos, C. P.; Noy, A.; Bakajin, O. *Science* **2006**, *312*, 1034–1037.

[8] Thomas, J. A.; McGaughey, A. J. H. *Journal Of Chemical Physics* **2008**, *128*, 084715.

[9] Jia, Y. X.; Li, H. L.; Wang, M.; Wu, L. Y.; Hu, Y. D. *Separation and Purification Technology* **2010**, *75*, 55–60.

[10] Corry, B. *Journal Of Physical Chemistry B* **2008**, *112*, 1427–1434.

[11] Murad, S.; Powles, J. G. *Journal Of Chemical Physics* **1993**, *99*, 7271–7272.

[12] Kim, K. S.; Davis, I. S.; Macpherson, P. A.; Pedley, T. J.; Hill, A. E. *Proceedings Of The Royal Society Of London Series A-Mathematical Physical And Engineering Sciences* **2005**, *461*, 273–296.

[13] Harder, E.; Walters, D. E.; Bodnar, Y. D.; Faibish, R. S.; Roux, B. *Journal Of Physical Chemistry B* **2009**, *113*, 10177–10182.

[14] Hughes, Z. E.; Gale, J. D. *Journal of Materials Chemistry* **2010**, *20*, 7788–7799.

[15] Raghunathan, A. V.; Aluru, N. R. *Physical Review Letters* **2006**, *97*, 024501.

[16] Suk, M. E.; Raghunathan, A. V.; Aluru, N. R. *Applied Physics Letters* **2008**, *92*, 133120.

[17] Werder, T.; Walther, J. H.; Jaffe, R. L.; Halicioglu, T.; Koumoutsakos, P. *Journal Of Physical Chemistry B* **2003**, *107*, 1345–1352.

[18] Allen, M. P.; Tildesley, D. *Computer simulation of liquids*; Clarendon Press, 1987.

[19] Dang, L. X.; Rice, J. E.; Caldwell, J.; Kollman, P. A. *Journal Of The American Chemical Society* **1991**, *113*, 2481–2486.

[20] Dang, L. X.; Kollman, P. A. *Journal Of Physical Chemistry* **1995**, *99*, 55–58.

[21] Plimpton, S. *Journal of Computational Physics* **1995**, *117*, 1–19.

[22] Hockney, R. W.; Eastwood, J. W. *Computer Simulation Using Particles*; Adam Hilger, Bristol, 1988.

[23] Berendsen, H. J. C.; Grigera, J.; Straatsma, T. P. *Journal Of Physical Chemistry* **1987**, *91*, 6269–6271.

[24] Callahan, K. M.; Casillas-Ituarte, N. N.; Roeselova, M.; Allen, H. C.; Tobias, D. J. *Journal of Physical Chemistry A* **2010**, *114*, 5141–5148.

[25] Raghunathan, A. V.; Aluru, N. R. *Applied Physics Letters* **2006**, *89*, 064107.

[26] Zeng, L.; Zuo, G. H.; Gong, X. J.; Lu, H. J.; Wang, C. L.; Wu, K. F.; Wan, R. Z. *Chinese Physics Letters* **2008**, *25*, 1486–1489.